

Short Communication

Application of conducting polymer poly (3,4-ethylenedioxythiophene)/reduced graphene oxide nanocomposite as sensor for determination of tyrosine in food

Xiuwen Wu^{1,2,*}, Miao Li², Xu Deng³

¹ School of Energy and Power Engineering, Xi'an Jiaotong University, Xi'an 710049, P.R.China

² Wuhan Gujin Technology Co.,Ltd, Wuhan, 430000, P.R.China

³ Shaanxi University of Chinese Medicine, XiXian New Area, 712046, P.R.China

*E-mail: wxw_whgkj@sina.com

Received: 21 July 2022 / Accepted: 16 September 2022 / Published: 10 October 2022

The goal of the ongoing research is to create an electrochemical sensor that can detect tyrosine in food that is stable, sensitive, and selective. This sensor will be built of a conducting polymer called poly (3,4,-dioxxythiophene) (PEDOT) and a reduced graphene oxide (rGO) nanocomposite. An electrodeposition method was used to create the glassy carbon electrode (GCE) modified with rGO-PEDOT nanocomposite. The electrodeposition of rGO-PEDOT on GCE was confirmed by SEM and EIS analysis. Electrochemical studies using DPV revealed that rGO and PEDOT nanostructures had a synergistic effect in promoting charge transfer as a sensitive and selective sensor with a linear range of 1 to 120 ng ml⁻¹. The detection limit and sensitivity were calculated to be 0.012 ng ml⁻¹ and 0.3578μA/ngml⁻¹, respectively. The usefulness and precision of rGO-PEDOT/GCE for determining tyrosine in prepared real samples from beans were explored. The proposed tyrosine sensor's practical viability was evaluated to estimate the level of tyrosine in genuine bean samples. The results showed that the recovery values (91.52% to 98.31%) and RSD values (2.26 % to 4.93%) were satisfactory. The results demonstrate that the developed tyrosine sensor has high precision, acceptable validity, and excellent application potential.

Keywords: Conducting polymer; Reduced graphene oxide; Nanocomposite; Tyrosine; Food samples; Electrochemical Sensor

1. INTRODUCTION

One of the amino acids required for the upkeep of a nutritional balance is tyrosine (Tyr) [1, 2]. Tyr levels in the body are related to a person's level of health [3, 4]. Tyr serves as a precursor for several hormones found in the central nervous system, including thyroxin, dopa, dopamine, noradrenalin, and adrenalin [5-7]. A person's body can produce tyr if they consume enough phenylalanine. Since phenylketonuria patients are unable to consume phenylalanine, they frequently

take tyrosine supplements [8, 9]. Several studies have found that eating foods high in Tyr, such as cheese, lamb, cattle, soybeans, pork, fish, poultry, beans, nuts, seeds, dairy, eggs, and whole grains, can help people remember things better under stress [10, 11]. In the lack of Tyr, several illnesses like hypochondrium, sadness, and other psychiatric illnesses might be seen [12-14]. Therefore, effective analytical methods are required for Tyr's assessment in food samples due to its nutritional value [15, 16]. Numerous analytical techniques have been published for the determination of Tyr, including chemiluminescence, fluorometric techniques, spectrometric testing, high performance liquid chromatography, and capillary electrophoresis [17-19]. However, the majority of these techniques are constrained by drawbacks including expense, length of analysis, and sample preparation [20, 21]. An easy, inexpensive, and quick method for analyzing physiologically and environmentally significant chemicals is by electrochemical methods [22, 23]. Sadly, amino acids perform poorly electrochemically on solid electrodes; as a result, chemical modifications are used to enhance their performance [24-26].

Because of their mechanical strength, conductance, abundance of surface functionality, ease of manufacturing, catalytic activity, and environmentally friendly nature, graphene-based conducting polymer materials have received attention in recent years for use in a variety of technological applications [27-29]. The thickness and length of the polymeric chains of these nanocomposites on a substrate can be adjusted depending on the needs of the application [30-32]. The PEDOT-graphene compound has attracted interest in a number of electrochemical devices, such as supercapacitors, tissue regeneration, and biosensors, among the other graphene-based polymeric composites which have been proposed [33-35]. It might be because the backbone of the poly (3,4,-dioxythiophene) (PEDOT) polymer efficiently interacts with charged dopants including reduced graphene oxide (rGO), allowing for the creation of nanocomposites with improved stability [36-38]. Previous research has confirmed that this nanocomposite performs better as an electrode modification than using a PEDOT matrix by itself. To the best of our knowledge, a small number of nanocomposites based on PEDOT graphene have been created for electrochemical sensing applications [39]. These studies are conducted to improve the detection limit for application electrochemical sensors in biological fluids, and the prepared sensors have been performed in a narrow and restricted linear range which limits further applications in pharmaceutical and food samples with a high level of Tyr. Therefore, in this study, a promising electrode matrix for such highly sensitive and selective sensing of Tyr is proposed using a rGO-PEDOT nanocomposite.

Electrocatalysts prefer rGO-PEDOT electrodes because of their electrical conductivity, large number of active sites, and unique surface functions. The manufactured differential pulsed voltammetry (DPV) sensor exhibits good sensitivity for detecting the three separations and purifications individually and great selectivity for usage in their simultaneous determination. The nanocomposite's fabrication is straightforward. The proposed electrode shows tremendous promise for usage in sensing applications for practical applications, according to a study of produced samples.

2. MATERIALS AND METHODS

Three electrodes—rGO, PEDOT, and rGO-PEDOT modified GCEs—were made. The Hummer's technique was used to create graphene oxide (GO) [40]. 20 mg of GO was combined with 20mL of water and sonicated for three hours to create the rGO. The resulting mixture was then given 0.5 g of NaBH₄, and it was continuously stirred for 15 hours. After the reaction was finished, ethanol and then water were used to wash the mixture. The processed black rGO was then dried under a vacuum at 50°C. An rGO/GCE was created by drop-casting approximately 10mL of the rGO distribution onto a polished GCE. The rGO-PEDOT/GCE was electrodeposited with PEDOT in 0.1M H₂SO₄ including 0.01M PEDOT during 100s at a fixed voltage of +0.9V. A PEDOT/GCE was created using the same procedure.

The prepared sample's morphology was examined using scanning electron microscopy (SEM). The electrochemical studies were conducted using an electrochemical device with a three-electrode setup. GCE served as the working-electrode, SCE served as the reference-electrode, and Pt wire served as the counter-electrode. Measurements were made using electrochemical impedance spectroscopy in the 0.1Hz to 10000Hz frequency range. GCE, rGO/GCE, and rGO-PEDOT/GCE were used as the working electrodes in a typical three-electrode electrochemical cell to perform differential pulse voltammetry (DPV) in electrochemical studies of materials under potential range of -0.4 to 0.2V into 0.1M phosphate buffer solutions (PBS) in scan rate of 10mVs⁻¹. PBS, that are composed of NaH₂PO₄ (98%) and H₃PO₄ (90%), were used as the electrolyte in electrochemical cells.

The approach described in [41] was used in the production of the real sample. Four common beans have been cut into individual pieces, processed in a blender, and given the designations E1, E2, E3, and E4. All pureed beans were then treated for 20 minutes with 1 cc of 0.1 M HCl (39%) and filtered. The pH was then brought down to 6.5 by centrifuging the 10 ml of filtered mixtures for 20 minutes before adding 12ml of 0.1M ammonia (29%) to the solutions. After being diluted with 2 mL of PBS, the supernatants were used as four prepared actual samples for tyrosine level measurement.

3. RESULTS AND DISCUSSION

The SEM picture of wavy and intertwined graphene oxide sheets is depicted in Figure 1a. Figure 1b shows the shale-like PEDOT structures are evenly scattered on the rGO. When PEDOT nanostructures are anchored to mesoporous graphene oxide sheets, a high porosity surface and a high specific surface area ratio are produced. The PEDOT nanoparticles are introduced between the rGO monolayers as a stabilizer to prevent sheet agglomeration [42-44].

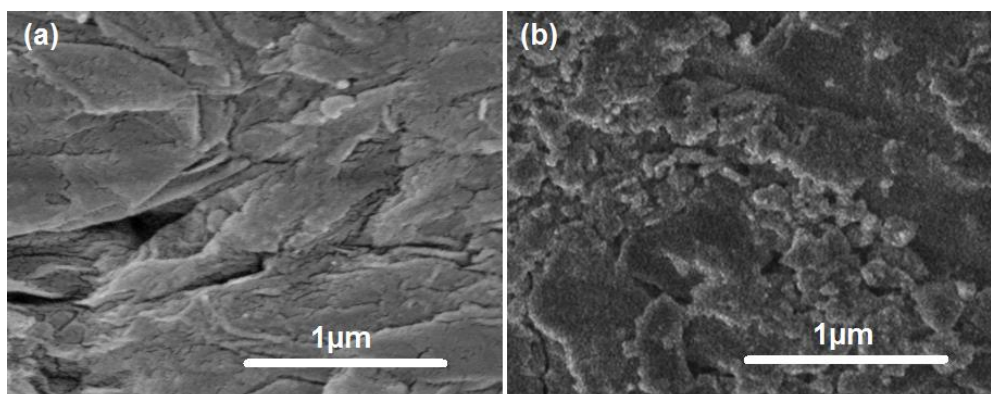


Figure 1. SEMs of (a) rGO sheets and (b) rGO-PEDOT nanocomposite

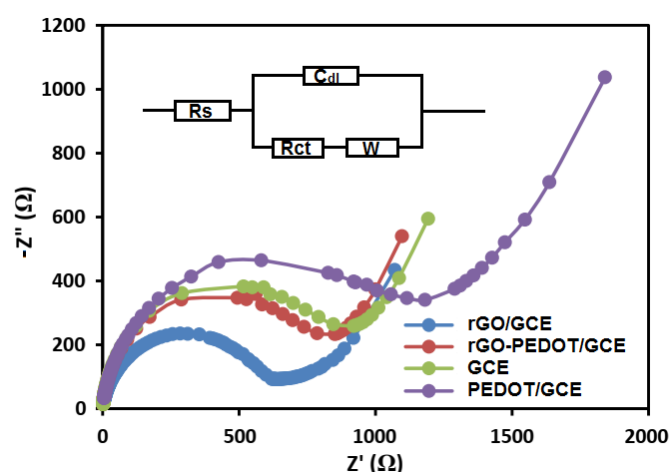


Figure 2. Nyquist diagrams of PEDOT, rGO and rGO-PEDOT nanocomposites modified GCE. Inset figure shows equivalent circuit model

Electrochemical impedance spectroscopy (EIS) was used to investigate the interfacial characteristics of the electrode materials. Figure 2 displays the Nyquist curves of four electrodes (uncoated GCE, PEDOT/GCE, rGO/GCE, and rGO-PEDOT/GCE) in 0.1M KCl with 10mM $K_4Fe(CN)_6$ and $K_3Fe(CN)_6$ on each electrode, respectively, at an applied AC voltage of 20mV. A semicircle inside the high frequency region associated with the charge, or transfer of electrons, with a diameter associated with the charge-transfer resistance (R_{ct}), as well as a linear section at the lower frequencies associated with the diffusion limited procedure are both visible on Nyquist curves of the electrodes [45-47]. When compared to the naked GCE, the changed electrodes showed observable variations in R_{ct} values, which amply demonstrated the efficacy of surface modification. The Randle equivalent circuit that was discovered and could be adapted to the impedance of each electrode is shown in the inset of Figure 2. The Randles circuit's R_{ct} and Warburg impedance were parallel to C_{dl} , producing the semicircle in Nyquist charts [48-50]. The basic GCE's R_{ct} value was around 1026 Ω . Due to the semiconducting properties of PEDOT film, after the GCE was altered with it, R_{ct} significantly rose to 1489 Ω . The high conductivity rGO surface layer was responsible for the R_{ct} values of rGO/GCE, which were approximately 685 Ω and significantly less than the naked GCE. R_{ct} slightly

increased to 848Ω when the rGO-PEDOT composites was used to alter the GCE [51, 52]. These findings imply that the GCE's surfaces were successfully used to create the rGO-PEDOT nanocomposite.

To determine the sensitivity, linear-range, and limit of detection of the rGO-PEDOT/GCE response to the injection of 1 ng mL^{-1} of tyrosine solution in potential range of -0.4 to 0.2 V at 10 mVs^{-1} , the following electrochemical tests were carried out using the DPV approach. Figure 3 shows DPVs and calibration plots for rGO-PEDOT/GCE after each injection of 1 ng mL^{-1} tyrosine solution, corresponding to a sensitivity of $0.3578\mu\text{A/ng mL}^{-1}$ and a limit of detection of 0.012 ng mL^{-1} .

Additional electrochemical tests were carried out in electrochemical cells with the addition of 10 ng mL^{-1} tyrosine solution in order to determine the linear-range of rGO-PEDOT/GCE toward tyrosine. The DPV response and calibrated plotted curve are displayed in Figure 4. It shows that the tyrosine measurement on rGO-PEDOT/GCE has an achieved linear range of $1\text{--}120\text{ ng mL}^{-1}$. The observed sensitivity, linear-range, and detection limit of rGO-PEDOT/GCE are also compared with those of other sensors for the measurement of tyrosine in the literature [53-55]. The comparison shows that the reported electrochemical biosensor in Table 1 and the rGO-PEDOT/GCE detecting properties are equivalent or superior. Additionally, high porosity, effective site, and enhanced surface area for rGO-PEDOT nanocomposites resulted in the broad linear range for tyrosine measurement [56-58]. Due to the synergistic effects of rGO and PEDOT nanostructures, it has been discovered that the fabrication of rGO-PEDOT composites on GCE displays a low detection limit with excellent linear range for tyrosine, which is comparable with the other nanostructured-based sensors [59-61]. According to studies, integrating rGO with PEDOT nanostructures in electrochemical sensors results in excellent benefits like improved mass-transport and sensitivity, lower detection thresholds, and quick electron-transfer kinetics into electrochemical reactions.

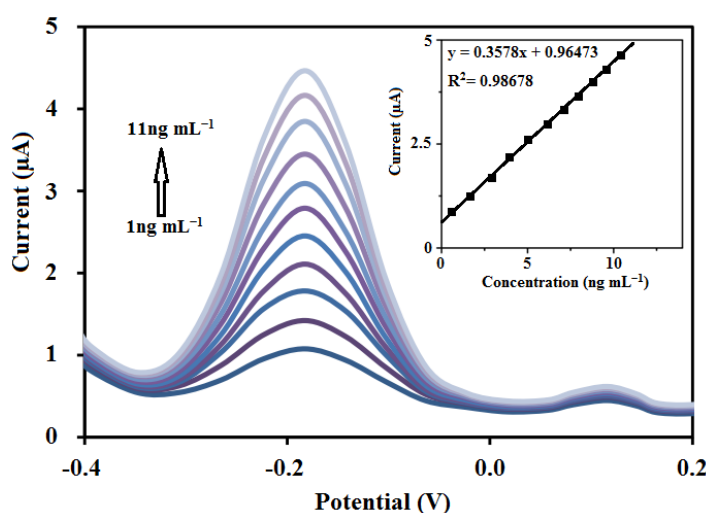


Figure 3. DPV response of rGO-PEDOT/GCE under potential range of -0.4 to 0.2 V into 0.1 M PBS solution in 10 mVs^{-1} for adding 1 ng mL^{-1} of tyrosine solution. Inset figure shows calibration curve

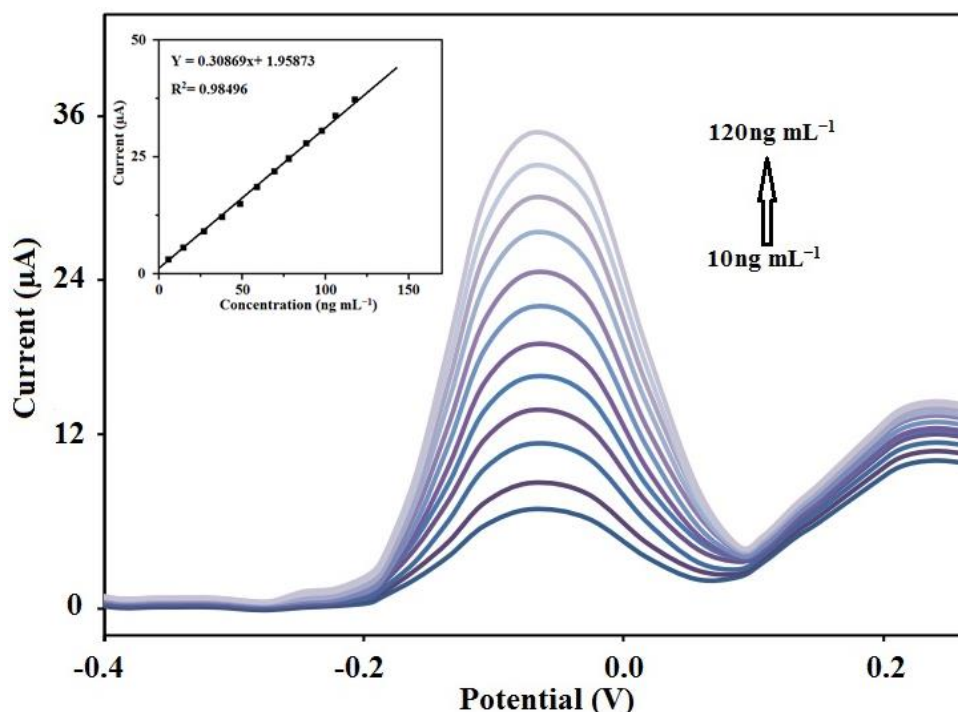


Figure 4. DPV response of rGO-PEDOT/GCE under potential range of -0.4 to 0.2V into 0.1M PBS solution in 10mVs^{-1} for adding 10ng mL^{-1} of tyrosine solution. Inset figure shows calibration curve

Table 1. Comparing rGO-PEDOT/GCE for tyrosine detection with various reported sensors

Electrode	Technique	Detection limit	Linear-range	Ref.
CuO/ β -CD/Nf/GCE	CV	$0.0082\ \mu\text{M}$	0.01 to $100\ \mu\text{M}$	[62]
MWCNTs-Nafion/GCE	CV	$0.8\ \mu\text{M}$	2.0– $120.0\ \mu\text{M}$	[63]
MIP/pTH/Au@ZIF-67/GCE	DPV	$7.9\ \text{nM}$	0.01- $4\ \mu\text{M}$	[64]
UT-g-C ₃ N ₄ /Ag	CV	$0.14\ \mu\text{M}$	1- $150\ \mu\text{M}$	[65]
Molecularly imprinted polymer	EIS	$6.63\ \text{pM}$	0.0001nM-1mM	[66]
GO-CS Modified Carbon-Based Electrodes	DPV	$5.86\ \mu\text{M}$	1- $100\ \mu\text{M}$	[67]
rGO-PEDOT/GCE	DPV	$0.012\ \text{nM}$	1- $120\ \text{nM}$	This work

For the purpose of examining the analytical application of the rGO-PEDOT/GCE to assess tyrosine using the conventional addition technique, four actual bean samples, designated as E1, E2, E3, and E4, were generated. rGO-PEDOT/GCE is dependable for the detection of tyrosine in actual samples, as shown by Table 2's satisfactory values for recovery within a range of 91.52%-98.31% and RSD within a range of 2.26%-4.93%.

Table 2. Analytical applicability of rGO-PEDOT/GCE to determine tyrosine in real specimens

Sample	Adding(μM)	Found(μM)	Recovery(%)	RSD(%)
E1	5.00	4.93	98.31	2.26
E2	10.00	9.66	91.52	3.74
E3	15.00	14.52	93.65	4.86
E4	20.00	19.78	97.64	4.93

4. CONCLUSION

In this study, an electrochemical sensor was used to detect tyrosine in food that was stable, sensitive, and selective. This sensor will be built from PEDOT and rGO nanocomposites. An electrodeposition method was used to create the GCE modified with rGO-PEDOT nanocomposite. The electrodeposition of rGO-PEDOT on GCE was confirmed by SEM and EIS analysis. Electrochemical studies using DPV revealed that rGO and PEDOT nanostructures had a synergistic effect in promoting charge transfer as a sensitive and selective sensor with a linear range of 1 to 120 ng ml⁻¹. The detection limit and sensitivity were calculated to be 0.012 ngml⁻¹ and 0.3578 $\mu\text{A}/\text{ngml}^{-1}$, respectively. The usefulness and precision of rGO-PEDOT/GCE for determining tyrosine in prepared real samples from beans were explored. To estimate the level of tyrosine in genuine bean samples, the proposed tyrosine sensor's practical viability was evaluated. The results showed that the recovery values (91.52% to 98.31%) and RSD values (2.26% to 4.93%) were satisfactory. The results demonstrate that the developed tyrosine sensor has high precision, acceptable validity, and excellent application potential.

ACKNOWLEDGEMENT

This work was sponsored in part by The Hubei Special program for Scientific and technological personnel enterprise cooperation.

References

1. K. Varmira, G. Mohammadi, M. Mahmoudi, R. Khodarahmi, K. Rashidi, M. Hedayati, H.C. Goicoechea and A.R. Jalalvand, *Talanta*, 183 (2018) 1.
2. H. Karimi-Maleh, H. Beitollahi, P.S. Kumar, S. Tajik, P.M. Jahani, F. Karimi, C. Karaman, Y. Vasseghian, M. Baghayeri and J. Rouhi, *Food and Chemical Toxicology*, (2022) 112961.
3. G. Luo, J. Xie, J. Liu, Q. Zhang, Y. Luo, M. Li, W. Zhou, K. Chen, Z. Li and P. Yang, *Chemical Engineering Journal*, 451 (2022) 138549.
4. F. Zhao, L. Song, Z. Peng, J. Yang, G. Luan, C. Chu, J. Ding, S. Feng, Y. Jing and Z. Xie, *Remote Sensing*, 13 (2021) 2129.
5. J.A. Gwin, D.D. Church, A. Hatch-McChesney, E.E. Howard, C.T. Carrigan, N.E. Murphy, M.A. Wilson, L.M. Margolis, J.W. Carbone and R.R. Wolfe, *Clinical Nutrition*, 40 (2021) 767.
6. H. Zhu and R. Zhao, *Vacuum*, 205 (2022) 111396.
7. M. Yang, C. Li, Y. Zhang, D. Jia, X. Zhang, Y. Hou, R. Li and J. Wang, *International Journal of Machine Tools and Manufacture*, 122 (2017) 55.
8. Y. Deng, L. Huang, C. Zhang, P. Xie, J. Cheng, X. Wang and L. Liu, *Industrial crops and products*, 148 (2020) 112331.

9. Y. Wu, Y. Zhao, X. Han, G. Jiang, J. Shi, P. Liu, M.Z. Khan, H. Huhtinen, J. Zhu and Z. Jin, *Materials Today Physics*, 18 (2021) 100400.
10. M.O. Omosebi, O.F. Osundahunsi and T.N. Fagbemi, *Journal of Food Biochemistry*, 42 (2018) e12508.
11. F. Zhao, S. Zhang, Q. Du, J. Ding, G. Luan and Z. Xie, *Socio-Economic Planning Sciences*, 78 (2021) 101066.
12. A. Parsa, N. Akbarzadeh-Torbati and H. Beitollahi, *International Journal of Electrochemical Science*, 14 (2019) 1556.
13. Z. Wang, L. Dai, J. Yao, T. Guo, D. Hrynsphan, S. Tatsiana and J. Chen, *Bioresource Technology*, 327 (2021) 124785.
14. H. Karimi-Maleh, C. Karaman, O. Karaman, F. Karimi, Y. Vasseghian, L. Fu, M. Baghayeri, J. Rouhi, P. Senthil Kumar and P.-L. Show, *Journal of Nanostructure in Chemistry*, (2022) 1.
15. X. Tang, J. Wu, W. Wu, Z. Zhang, W. Zhang, Q. Zhang, W. Zhang, X. Chen and P. Li, *Analytical chemistry*, 92 (2020) 3563.
16. Z. Zhu, Y. Wu and J. Han, *Frontiers in Earth Science*, (2022) 1424.
17. N.F. Atta, A. Galal and Y.M. Ahmed, *Journal of The Electrochemical Society*, 166 (2019) B623.
18. H. Chen and Q. Wang, *Biological Reviews*, 96 (2021) 2373.
19. Y. Yang, H. Zhu, X. Xu, L. Bao, Y. Wang, H. Lin and C. Zheng, *Microporous and Mesoporous Materials*, 324 (2021) 111289.
20. M. Cheng, Y. Cui, X. Yan, R. Zhang, J. Wang and X. Wang, *Food Hydrocolloids*, 124 (2022) 107225.
21. Y. Wang, C. Li, Y. Zhang, M. Yang, B. Li, L. Dong and J. Wang, *International Journal of Precision Engineering and Manufacturing-Green Technology*, 5 (2018) 327.
22. C. Raril, J.G. Manjunatha, D.K. Ravishankar, S. Fattepur, G. Siddaraju and L. Nanjundaswamy, *Surface Engineering and Applied Electrochemistry*, 56 (2020) 415.
23. T. Li, D. Shang, S. Gao, B. Wang, H. Kong, G. Yang, W. Shu, P. Xu and G. Wei, *Biosensors*, 12 (2022) 314.
24. J. Zhang, C. Li, Y. Zhang, M. Yang, D. Jia, G. Liu, Y. Hou, R. Li, N. Zhang and Q. Wu, *Journal of cleaner production*, 193 (2018) 236.
25. D. Zhenjing, L. Changhe, Y. Zhang, D. Lan, B. Xiufang, Y. Min, J. Dongzhou, L. Runze, C. Huajun and X. Xuefeng, *Chinese Journal of Aeronautics*, 34 (2021) 33.
26. C. Liu and J. Rouhi, *RSC Advances*, 11 (2021) 9933.
27. D. Saidina, N. Eawwiboonthanakit, M. Mariatti, S. Fontana and C. Hérold, *Journal of Electronic Materials*, 48 (2019) 3428.
28. T. Li, W. Yin, S. Gao, Y. Sun, P. Xu, S. Wu, H. Kong, G. Yang and G. Wei, *Nanomaterials*, 12 (2022) 982.
29. L. Nan, C. Yalan, L. Jixiang, O. Dujuan, D. Wenhui, J. Rouhi and M. Mustapha, *RSC Advances*, 10 (2020) 27923.
30. J. Liu, T. Li, H. Zhang, W. Zhao, L. Qu, S. Chen and S. Wu, *Materials Today Bio*, 14 (2022) 100243.
31. L. Tang, Y. Zhang, C. Li, Z. Zhou, X. Nie, Y. Chen, H. Cao, B. Liu, N. Zhang and Z. Said, *Chinese Journal of Mechanical Engineering*, 35 (2022) 1.
32. M. Yang, C. Li, Y. Zhang, Y. Wang, B. Li, D. Jia, Y. Hou and R. Li, *Applied Thermal Engineering*, 126 (2017) 525.
33. M. Suominen, P. Damlin and C. Kvarnström, *Electrochimica Acta*, 307 (2019) 214.
34. Z. Ke, Y. Bai, Y. Bai, Y. Chu, S. Gu, X. Xiang, Y. Ding and X. Zhou, *Food Chemistry*, 377 (2022) 131932.
35. Y. Yang, M. Yang, C. Li, R. Li, Z. Said, H.M. Ali and S. Sharma, *Frontiers of Mechanical Engineering*, (2022) 1.

36. M. Heydari Gharahcheshmeh, M.M. Tavakoli, E.F. Gleason, M.T. Robinson, J. Kong and K.K. Gleason, *Science advances*, 5 (2019) eaay0414.
37. G. Liu, R. Nie, Y. Liu and A. Mehmood, *Science of the Total Environment*, 825 (2022) 154058.
38. J. Rouhi, S. Mahmud, S.D. Hutagalung and N. Naderi, *Electronics letters*, 48 (2012) 712.
39. M. Soni, M. Bhattacharjee, M. Ntagios and R. Dahiya, *IEEE Sensors Journal*, 20 (2020) 7525.
40. W.S. Hummers Jr and R.E. Offeman, *Journal of the american chemical society*, 80 (1958) 1339.
41. L. Yan, X. Yan, H. Li, X. Zhang, M. Wang, S. Fu, G. Zhang, C. Qian, H. Yang and J. Han, *Microchemical Journal*, 157 (2020) 105016.
42. L. Valenzuela, A. Iglesias-Juez, B. Bachiller-Baeza, M. Faraldos, A. Bahamonde and R. Rosal, *Journal of Materials Chemistry B*, 2020 (2020) 1.
43. J. Wang, T. Tsuzuki, B. Tang, X. Hou, L. Sun and X. Wang, *ACS Applied Materials & Interfaces*, 4 (2012) 3084.
44. C. Xin, L. Changhe, D. Wenfeng, C. Yun, M. Cong, X. Xuefeng, L. Bo, W. Dazhong, H.N. Li and Y. Zhang, *Chinese Journal of Aeronautics*, (2021) 1.
45. J. Recio-Hernandez, M. Galicia-García, H. Silva-Jiménez, R. Malpica-Calderón and E.G. Ordoñez-Casanova, *International Journal of Electrochemical Science*, 16 (2021) 1.
46. Y. Xu, X. Chen, H. Zhang, F. Yang, L. Tong, Y. Yang, D. Yan, A. Yang, M. Yu and Z. Liu, *International Journal of Energy Research*, (2022) 1.
47. X. Wu, C. Li, Z. Zhou, X. Nie, Y. Chen, Y. Zhang, H. Cao, B. Liu, N. Zhang and Z. Said, *The International Journal of Advanced Manufacturing Technology*, 117 (2021) 2565.
48. J. Eveness, L. Cao, J. Kiely and R. Luxton, *Journal of Electroanalytical Chemistry*, 906 (2022) 116003.
49. Y. Chen, J. Long, B. Xie, Y. Kuang, X. Chen, M. Hou, J. Gao, H. Liu, Y. He and C.-P. Wong, *ACS Applied Materials & Interfaces*, 14 (2022) 4647.
50. Z. Said, M. Ghodbane, B. Boumeddane, A.K. Tiwari, L.S. Sundar, C. Li, N. Aslfattahi and E. Bellos, *Solar Energy Materials and Solar Cells*, 239 (2022) 111633.
51. H. Karimi-Maleh, R. Darabi, M. Shabani-Nooshabadi, M. Baghayeri, F. Karimi, J. Rouhi, M. Alizadeh, O. Karaman, Y. Vasseghian and C. Karaman, *Food and Chemical Toxicology*, 162 (2022) 112907.
52. S. Changaei, J. Zamir-Anvari, N.-S. Heydari, S.G. Zamharir, M. Arshadi, B. Bahrami, J. Rouhi and R. Karimzadeh, *Journal of Electronic Materials*, 48 (2019) 6216.
53. S.T. Yang, X.Y. Li, T.L. Yu, J. Wang, H. Fang, F. Nie, B. He, L. Zhao, W.M. Lü and S.S. Yan, *Advanced Functional Materials*, 32 (2022) 2202366.
54. T. Gao, C. Li, Y. Wang, X. Liu, Q. An, H.N. Li, Y. Zhang, H. Cao, B. Liu and D. Wang, *Composite Structures*, 286 (2022) 115232.
55. J. Rouhi, S. Mahmud, S.D. Hutagalung, N. Naderi, S. Kakooei and M.J. Abdullah, *Semiconductor Science and Technology*, 27 (2012) 065001.
56. L. Sheng, Z. Li, A. Meng and Q. Xu, *Sensors and Actuators B: Chemical*, 254 (2018) 1206.
57. Y. Sun, J. Li, L. Zhu and L. Jiang, *Current Opinion in Food Science*, 44 (2022) 100813.
58. H. Maleh, M. Alizadeh, F. Karimi, M. Baghayeri, L. Fu, J. Rouhi, C. Karaman, O. Karaman and R. Boukherroub, *Chemosphere*, (2021) 132928.
59. S. Gupta, A. Tiwari, U. Jain and N. Chauhan, *Materials Science and Engineering: C*, 103 (2019) 109733.
60. L. Yang, H. Huang, Z. Xi, L. Zheng, S. Xu, G. Tian, Y. Zhai, F. Guo, L. Kong and Y. Wang, *Nature communications*, 13 (2022) 1.
61. B. Li, C. Li, Y. Zhang, Y. Wang, D. Jia and M. Yang, *Chinese Journal of Aeronautics*, 29 (2016) 1084.
62. A. Karthika, D.R. Rosaline, S. Inbanathan, A. Suganthi and M. Rajarajan, *Journal of Physics and Chemistry of Solids*, 136 (2020) 109145.

63. Z.-Y. Li, D.-Y. Gao, Z.-Y. Wu and S. Zhao, *RSC advances*, 10 (2020) 14218.
64. B. Chen, Y. Zhang, L. Lin, H. Chen and M. Zhao, *Journal of Electroanalytical Chemistry*, 863 (2020) 114052.
65. J. Zou, D. Mao, A.T.S. Wee and J. Jiang, *Applied Surface Science*, 467 (2019) 608.
66. S. Roy, S. Nagabooshanam, S. Wadhwa, N. Chauhan, A. Mathur, S.A. Khan and J. Davis, *Electrochemistry Communications*, 117 (2020) 106782.
67. S. Dervin, P. Ganguly and R.S. Dahiya, *IEEE Sensors Journal*, 21 (2021) 26226.

© 2022 The Authors. Published by ESG (www.electrochemsci.org). This article is an open access article distributed under the terms and conditions of the Creative Commons Attribution license (<http://creativecommons.org/licenses/by/4.0/>).